

## Accepted Article

**Title:** Dibenzoarsepins: Planarization of  $8\pi$ -Electron System in the Lowest Singlet Excited State

**Authors:** Ikuo Kawashima, Hiroaki Imoto, Masatoshi Ishida, Hiroyuki Furuta, Shunsuke Yamamoto, Masaya Mitsuishi, Susumu Tanaka, Toshiki Fujii, and Kensuke Naka

This manuscript has been accepted after peer review and appears as an Accepted Article online prior to editing, proofing, and formal publication of the final Version of Record (VoR). This work is currently citable by using the Digital Object Identifier (DOI) given below. The VoR will be published online in Early View as soon as possible and may be different to this Accepted Article as a result of editing. Readers should obtain the VoR from the journal website shown below when it is published to ensure accuracy of information. The authors are responsible for the content of this Accepted Article.

**To be cited as:** *Angew. Chem. Int. Ed.* 10.1002/anie.201904882  
*Angew. Chem.* 10.1002/ange.201904882

**Link to VoR:** <http://dx.doi.org/10.1002/anie.201904882>  
<http://dx.doi.org/10.1002/ange.201904882>

## COMMUNICATION

Dibenzoarsepins: Planarization of 8 $\pi$ -Electron System in the Lowest Singlet Excited StateIkuo Kawashima,<sup>[a]</sup> Hiroaki Imoto,<sup>[a]</sup> Masatoshi Ishida,<sup>[b]</sup> Hiroyuki Furuta,<sup>[b]</sup> Shunsuke Yamamoto,<sup>[c]</sup> Masaya Mitsuishi,<sup>[c]</sup> Susumu Tanaka,<sup>[a]</sup> Toshiki Fujii,<sup>[a]</sup> and Kensuke Naka\*<sup>[a]</sup>

**Abstract:** Dibenzo[*b,f*]arsepins, **3-Me** and **3-Ph**, possessing severely distorted cores as compared to other heteropin families, were synthesized. These derivatives exhibited dual photoluminescence in the green-to-red region (500–700 nm) and the near-ultraviolet region (<380 nm), which could be attributed to the planarization of the arsepin cores in the lowest singlet excited ( $S_1$ ) states. The computational approach for the assessment of the aromatic indices revealed that **3-Me** and **3-Ph** show aromaticity ( $8\pi$  system) in the  $S_1$  states according to Baird's rule. The lone pair electrons of the arsenic atoms played a crucial role in the aromaticity in the  $S_1$  states.

Heteropins have seven-membered cycloheptatriene cores bridged by a heteroatom instead of an  $sp^3$  carbon atom, and their conformations and electronic features, reflecting the nature of the incorporated elements, have received much attention (Figure 1).<sup>[1–6]</sup> Carbon group heteropins such as cycloheptatriene and silepin have nonconjugated cores with a boat-like conformation, and due to the low energy barrier, rapidly undergo boat-to-boat ring inversion via a planar conformation.<sup>[1]</sup> The boron group heteropins (e.g., borepin,<sup>[2]</sup> aluminepin,<sup>[3]</sup> and gallepin<sup>[4]</sup>) possess isoelectronic structures with the tropylium ion and adopt the planar conformation with a  $6\pi$ -aromatic system at the heteropin core in the  $S_0$  states.<sup>[2a,3,4b]</sup> In contrast, chalcogen-based heteropins (e.g., oxepin and thiepin), which formally have an  $8\pi$ -electron circuit, avoid the unstable antiaromatic structures by adopting the distorted conformation in the  $S_0$  states. However, upon photoexcitation, conformational planarization in the lowest singlet excited state ( $S_1$ ) was predicted based on the photochemical reactivity of the compounds.<sup>[5]</sup> Ottosson suggested that this planarization is attributed to the Baird aromaticity rule.<sup>[7]</sup>

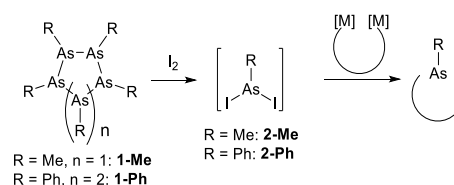
The concept of excited-state aromaticity according to Baird's rule is applicable to predict the photochemical properties of cyclic  $4n$  and  $4n+2$   $\pi$ -electron systems in their excited states.<sup>[8]</sup> Among them, the  $8\pi$  annulenic cyclooctatetraene (COT) systems, which are utilized as photoresponsive materials owing to their flapping motions upon photoexcitation, have been widely studied in the fields of structural and computational chemistry.<sup>[9]</sup> In-depth investigations on seven-membered heteropins with  $8\pi$ -electron

systems, which are constructed by the overlap of the lone pair electrons of their heteroatoms, should be of interest in terms of structural transformation in the excited state.<sup>[10]</sup>

	Group 13 (X = B, Al, Ga)	14	15 (Y = N, P, As)	16 (Z = O, S)
Conformation ( $S_0$ )	Planar	Bent	Bent	Bent
Electron system	$6\pi$	$6\pi$	$8\pi$	$8\pi$
Hückel aromaticity	Aromatic	Nonaromatic	Antiaromatic (N) Nonaromatic (P, As)	Antiaromatic
Baird aromaticity	Not investigated	Not investigated	Not investigated	Suggested

**Figure 1.** Schematic representation of the conformation and electron system of various heteropins. The corresponding aromaticity in the ground and excited states is also summarized.

Judging from the results of chalcogen-based heteropins, which have  $8\pi$ -electron systems including the lone pair one, the pnictogen group is suitable for realizing Baird aromaticity due to its lone pairs. For example, dibenzo[*b,f*]phosphepin has been reported to adopt a boat-like bent conformation.<sup>[6]</sup> Among the pnictogen group heteropins, arsepin, an arsenic analog of heteropin, is beneficial for photodriven planarization because the trivalent arsenic atom in the macrocycle has a lone pair electron that is chemically inert in air, as opposed to the air-sensitive phosphepin analogs.<sup>[11]</sup> However, despite the successful synthesis of arsepins, their conformation, optical properties, and aromatic character have not been elucidated in detail yet.<sup>[12]</sup> The main obstacle to experimental studies on arsepins is the high intrinsic toxicity and volatility of the precursor, arsenic dichloride.<sup>[11d,13]</sup> Recently, we have developed simple synthetic methodologies using cyclooligoarsines such as pentamethylpentacycloarsine (**1-Me**) and hexaphenylhexacycloarsine (**1-Ph**)<sup>[14]</sup> as shown in Scheme 1.<sup>[15]</sup> When the As–As bonds of these cyclooligoarsines are cleaved, reactive species such as radicals, electrophiles, and nucleophiles are generated *in situ*.<sup>[16]</sup> Diiodoarsines (**2-Me** and **2-Ph**) were then prepared by the addition of iodine to the cyclooligoarsines, and could be used for the construction of the cyclic arsepin core with a dilithio intermediate.<sup>[16c]</sup>



**Scheme 1.** Easy and safe As–C bond formation via *in situ* generation of diiodoarsines from cyclooligoarsines.

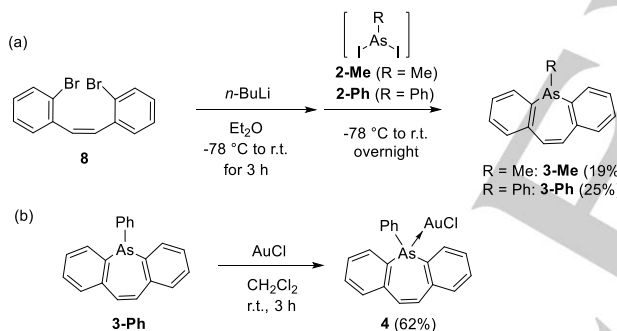
- [a] I. Kawashima, Dr. H. Imoto, S. Tanaka, T. Fujii, Prof. Dr. K. Naka  
Faculty of Molecular Chemistry and Engineering, Graduate School of Science and Technology, Kyoto Institute of Technology  
Goshokaido-cho, Matsugasaki, Sakyo-ku, Kyoto 606-8585 (Japan)  
E-mail: kenaka@kit.ac.jp
- [b] Dr. M. Ishida, Prof. Dr. H. Furuta  
Department of Chemistry and Biochemistry, Graduate School of Engineering and Center for Molecular System, Kyushu University  
744 Moto-oka, Nishi-ku, Fukuoka 819-0395 (Japan)
- [c] Dr. S. Yamamoto, Prof. Dr. M. Mitsuishi  
Institute of Multidisciplinary Research for Advanced Materials (IMRAM), Tohoku University  
2-1-1 Katahira, Aoba-ku, Sendai 980-8577 (Japan)

Supporting information for this article is given via a link at the end of the document.

## COMMUNICATION

Herein, we report the synthesis of the new dibenzo[*b,f*]arsepin derivatives (**3-Me** and **3-Ph**) and their X-ray crystallographic structures. The photophysical properties were examined in detail to evaluate the conformational dynamics in their excited states. Furthermore, computational calculations were conducted to assess the aromatic character of these derivatives in the  $S_1$  states using nucleus-independent chemical shift (NICS), harmonic oscillator model of heterocyclic electron delocalization (HOMHED) index, and anisotropy of the induced current density (ACID) plot.

Compounds **3-Me** and **3-Ph** were synthesized as shown in Scheme 2a. Cyclooligoarsines **1-Me** and **1-Ph** were mixed with iodine in diethyl ether at 25 °C to prepare diiodoarsines **2-Me** and **2-Ph**, respectively, which were directly used for the subsequent reaction. The resulting solution was reacted with the 2,2'-dilithio-Z-stilbene intermediate generated from 2,2'-dibromo-Z-stilbene<sup>[3,17]</sup> at -78 °C. The reaction mixture was then allowed to warm to room temperature and stirred overnight to afford arsepins **3-Me** and **3-Ph** in 19% and 25% yields, respectively. The arsepins were stable; no oxidation or decomposition was observed even after storage in the solid state under ambient conditions for more than one month. The lone pairs on the arsenic atom could be utilized as a donor site for complexation; gold(I) metalation of **3-Ph** afforded adduct complex **4** in 62% yield (Scheme 2b). Single crystals of **3-Me**, **3-Ph**, and **4** suitable for the analyses were prepared by recrystallization from  $\text{CH}_2\text{Cl}_2$  and methanol or hexane by slow diffusion at -18 °C.



**Scheme 2.** Synthesis of (a) arsepin derivatives **3-Me** and **3-Ph**, and (b) gold(I) chloride complex (**4**).

The X-ray crystallographic structures and data for **3-Me**, **3-Ph**, and **4** are summarized in Figure 2 and Tables S1–S3.<sup>[18]</sup> The seven-membered arsepin cores for **3-Me** and **3-Ph** adopted a boat-like conformation. The sum of the inner angles of the seven-membered arsepin cores for **3-Me** (839.0(17)°) and **3-Ph** (846.2(6)°) were much smaller than that of the planar heptagon model (900°). These angles were also significantly smaller than those of the other dibenzoheteropins (856°–899°) as shown in Table S4,<sup>[2a,3,4b,6b,19]</sup> indicating that **3-Me** and **3-Ph** had the most distorted cores among the reported heteropins. The As–C bond lengths were also significantly longer (1.93–1.96 Å) than those of the other heteropins.<sup>[2a,3,4b,6b,19]</sup> The sum of the bond angles (C1–As–C14, C1–As–C15, and C14–As–C15) around the arsenic atoms was 295.4(5)° for **3-Me** and 299.1(2)° for **3-Ph**, suggesting that the arsenic atoms had a trigonal pyramidal geometry. The bent angles,  $\theta_1$  and  $\theta_2$ , were remarkably large for

both **3-Me** ( $\theta_1 = 34.0^\circ$ ,  $\theta_2 = 55.4^\circ$ ) and **3-Ph** ( $\theta_1 = 32.2^\circ$ ,  $\theta_2 = 52.5^\circ$ ) compared with other dibenzoheteropins (Table S4). The phenyl ring in **3-Ph** was oriented perpendicularly to the heterocyclic double bond of the heteropin core, in contrast to the case of the phosphepin derivatives.<sup>[6]</sup> Notably, bond alteration at the arsepin cores was observed for **3-Me** and **3-Ph**. The specific C7–C8 bond lengths were 1.33(2) Å (**3-Me**) and 1.330(4) Å (**3-Ph**), respectively, which were identical to the typical carbon-carbon double bond. The  $^1\text{H-NMR}$  spectra of **3-Me** and **3-Ph** supported the alkene character; the signals observed at 7.07 ppm (**3-Me**) and 6.80 ppm (**3-Ph**) could be attributed to the internal alkenes.

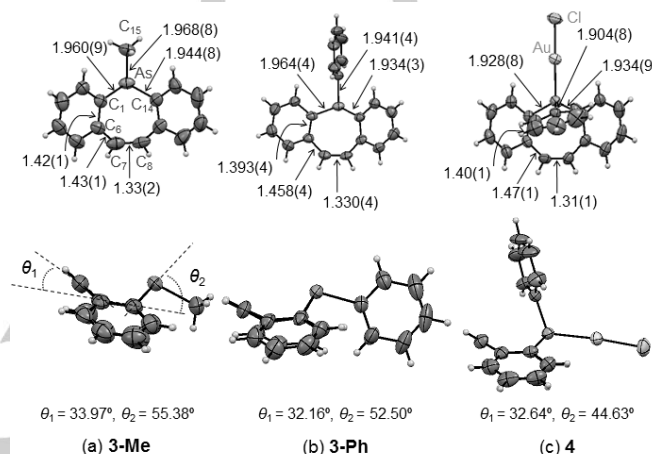


**Figure 2.** ORTEP drawings of (a) **3-Me**, (b) **3-Ph**, and (c) **4**. Top views (top) and side views (bottom) are shown (50% probability for thermal ellipsoids). Selected bond lengths (Å) and angles are shown. Crystallographic data are provided in Tables S1–S3.

The crystal structure of **4** indicated that the phenyl ring was positioned above the arsepin core plane and that the tetrahedral arsepin atom was coordinated to the gold(I) chloride unit in a monodentate fashion. The sum of the C–As–C bond angles (316.8(6)°) was larger than that for **3-Ph**, resulting in enhanced planarity of the arsepin core as the electronic repulsion between the lone pair and As–C bonds was alleviated by the coordination.

**Table 1.** Photophysical data for **3-Me**, **3-Ph**, and **4**.

	$\text{CHCl}_3$ solution <sup>a</sup>					Solid	
	$\lambda_{\text{abs}}^b$ /nm	$\lambda_{\text{em}}^c$ /nm	$\Phi_{\text{PL}}^d$	$\tau^e$ /ns	$\tau^f$ /ns	$\lambda_{\text{em}}^c$ /nm	$\Phi_{\text{PL}}^d$
<b>3-Me</b>	250	364	ND <sup>g</sup>	0.38	0.39	424	0.03
	288	584					
<b>3-Ph</b>	245	371	ND <sup>g</sup>	1.00	2.30	488	0.06
	296	557					
<b>4</b>	239	375	< 0.01	0.12	ND <sup>g</sup>	383	< 0.01
	301						

<sup>a</sup> $\text{CHCl}_3$  solution ( $1.0 \times 10^{-4}$  M) in air at room temperature. <sup>b</sup>Absorption maxima. <sup>c</sup>Emission maxima (excited at the excitation maxima). <sup>d</sup>Absolute quantum yields. <sup>e</sup>Fluorescence lifetime monitored feedback at 364 nm for **3-Me**, 371 nm for **3-Ph**, and 375 nm for **4**. <sup>f</sup>Fluorescence lifetime monitored feedback at 584 nm for **3-Me** and 557 nm for **3-Ph**. <sup>g</sup>Not determined.

UV-vis absorption (Figure S7) and photoluminescence (PL) spectra (Figure 3a-c) of **3-Me**, **3-Ph**, and **4** were measured in  $\text{CHCl}_3$ , and their photophysical data are summarized in Table 1.

## COMMUNICATION

Intense bands around 250 nm and relatively broad bands around 300 nm were observed in the absorption spectra for both **3-Me** and **3-Ph**. To gain insight into the vertical transition features of **3-Me** and **3-Ph**, density functional theory (DFT) calculations with (U)B3LYP functional and Grimme's dispersion correction, B3LYP-D3/6-31+G(d,p), were performed. The calculations well reproduced the crystal structures, which revealed the distorted tub-shaped arsepin cores of **3-Me** and **3-Ph** (*vide infra*, Figures S17–S18, Table S6). Time-dependent (TD) DFT calculations for **3-Me** and **3-Ph** revealed that the characteristic transitions with the lowest energy,  $S_0 \rightarrow S_1$  (323 nm and 336 nm, respectively), assigned as HOMO–LUMO transitions had relatively smaller oscillator strengths ( $f$ ) of 0.0217 and 0.0205, respectively (Figure S16, Table S5). The second intense bands could be visualized as the contribution of the HOMO-1–LUMO transitions, for both the compounds (Table S5).

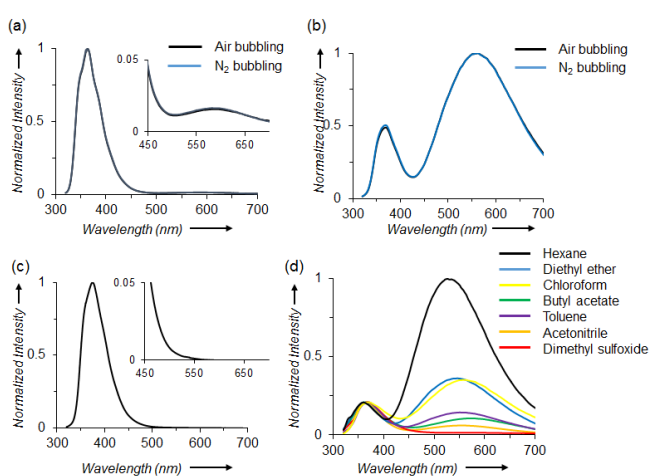


**Figure 3.** PL spectra ( $1.0 \times 10^{-4}$  M, 298 K) of (a) **3-Me**, (b) **3-Ph**, and (c) **4** in CHCl<sub>3</sub> after air bubbling (black lines) and N<sub>2</sub> bubbling (blue lines), and (d) **3-Ph** in various solvents.

Upon photoexcitation, arsepins **3-Me** (Figure 3a) and **3-Ph** (Figure 3b) excited at 288 nm and 296 nm, respectively, showed PL bands with large Stokes shifts of 7249 cm<sup>-1</sup> and 6830 cm<sup>-1</sup>, respectively. Concomitantly, broad bands were observed in the green-to-red region (500–700 nm).<sup>[20]</sup> The intensities of the longer-wavelength emissions were dependent on the solvent used; high emission intensity was observed in less polar solvents such as *n*-hexane (Figures 3d, S13) because the planar structure was less polar than the bent structure in the  $S_1$  state, as discussed below. When the arsepins were dispersed in the poly(methyl methacrylate) matrix (Figure S10), the longer-wavelength emission bands were diminished. Furthermore, we measured the PL spectra of **3-Ph** in various alkanes to investigate the effect of solvent viscosity. The higher the viscosity, the lower the relative intensity of the longer wavelength emission (Figure S14). These results imply that the structural relaxation toward the planarization was impeded by PMMA or viscous solvent matrix in the  $S_1$  state. We estimate the activation energy ( $\Delta E_a$ ) of the structural relaxation from the Franck-Condon state to the relaxed singlet state by the Stevens–Ban plot<sup>[21]</sup> of **3-Ph** in 2-methyltetrahydrofuran (Figure S15). The PL spectra of **3-Ph** were

measured from 145 K to 300 K, and the estimated  $\Delta E_a$  was 3.2 kJ/mol, meaning that the structural relaxation in the  $S_1$  state can occur at room temperature.

The fluorescence lifetime ( $\tau$ ) of **3-Ph** probed at 371 nm was fitted by the sum of two exponential decays to be 0.30 ns (99%) and 4.92 ns (1%) (Figure S8).<sup>[22]</sup> The exponential decay in the blue wavelength region was rapid, in contrast, the decay constants measured at longer wavelength (557 nm) with single exponential fitting were higher ( $\tau = 2.30$  ns). Time-resolved fluorescence spectrum for **3-Ph** in CHCl<sub>3</sub> revealed that the weak fluorescence band in the longer-wavelength region appeared during the decay of the intense emission band around 400 nm (Figure S12). These results suggested that the slow component in emission was ascribed to the conformational relaxation from the Franck-Condon state to the relaxed singlet state. Under anaerobic conditions, no phosphorescence was detected in CHCl<sub>3</sub>.<sup>[23]</sup> Additionally, no such conformational change occurred in the excited state of **4** owing to the geometrical restriction at the tetrahedral arsine atom, as inferred from the absence of longer-wavelength emissions (Figure 3c) and the single exponential fluorescence decay profile (Figure S8).

The planarization of the cores was demonstrated by the  $S_1$ -excited state calculations (Figures 4, S21).<sup>[24]</sup> The energy profiles of the  $S_0$  and  $S_1$  species for **3-Me** and **3-Ph** indicated that the decrease in the torsion angle between the mean planes of the two benzene rings led to a monotonic decrease in the energies in the  $S_1$  state. The distinct low energy emissions were predicted by TDDFT calculations ( $\lambda_{em}$  of 634 nm for **3-Me** and 650 nm for **3-Ph**). The higher energy fluorescence around 360–370 nm was thus attributed to the vertical transition, based on the Franck-Condon principle, from the  $S_1$  to  $S_0$  states for **3-Me** and **3-Ph**, while the fluorescence observed in the longer wavelength regions could be derived from the transition geometry from the structurally relaxed  $S_1$  to the  $S_0$  states. The calculated excited state dipole moments ( $\mu_{ES}$ ) were slightly decreased upon planarization for both the compounds (Figures 4, S21), which suggested that the relaxed conformers were partially favored in less polar solvents such as *n*-hexane, as observed in Figures 3d and S13.

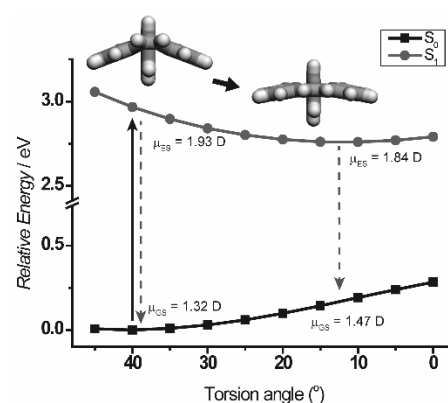


**Figure 4.** Energy diagram for  $S_0$  and  $S_1$  states of **3-Ph** by changing the torsion angle. Solid arrow stands for absorption process and dashed arrows for emission. The calculated dipole moments,  $\mu_{ES}$  (excited state) and  $\mu_{GS}$  (ground state), are provided.

## COMMUNICATION

Given that the arsepins adopt a quasi-planar conformation in the excited states after the structural relaxation, the arsepin cores possessing  $8\pi$ -conjugated systems, including the lone pair electrons on the arsenic atoms, would exhibit reversal of aromaticity in the  $S_1$  states according to Baird's rule. To evaluate the distinct aromaticity of **3-Me** and **3-Ph** in the  $S_1$  states, we performed calculations with the B3LYP-D3 functional (Figures S24–S27). As mentioned, both **3-Me** and **3-Ph** adopted bent geometries in the  $S_0$  states, and thus showed non-aromatic character, as inferred from the ACID plots, revealing the disconnected electron conjugation between the arsine and the adjacent carbons on the arsepin core (Figures S24–S25). In addition, the HOMHED values<sup>[25]</sup> of the arsepin cores were small (0.37 and 0.28 for **3-Me** and **3-Ph**, respectively) due to the significant bond length alteration of the  $8\pi$ -conjugated systems.<sup>[26]</sup> The NICS(1) values that were nearly zero at the arsepin cores also supported this conclusion (Table 2).

In turn, the arsepin cores of **3-Me** and **3-Ph** adopted a coplanar structure in the  $S_1$  states (*vide supra*), and the C1/C14–As bond lengths were estimated to be significantly shorter than those of the ground-state species (Figures S20–S21, Table S7).<sup>[27]</sup> In addition, the C7–C8 bonds were longer in the  $S_1$  states. Therefore, the HOMHED values of the flattened arsepin cores were estimated to be 0.89 for **3-Me** and 0.90 for **3-Ph** (Table 2), which could be attributed to the effective  $\pi$ -conjugation in the arsepin cores in the  $S_1$  excited states. This indicated the reversal of aromaticity based on Baird's rule. Moreover, the NICS plot scanned along the molecular z-axis showed moderate aromatic character for the arsepin cores as evident from the negative NICS(1) values above the center of the rings (e.g., –6.7 ppm and –9.3 ppm, respectively), although the gauge independent atomic orbital (GIAO) method was applied to the virtually constructed excited state structures in this calculation. The ACID plots represented clockwise ring currents on the arsepin rings as well as the adjacent benzene units for both **3-Me** and **3-Ph** (Figures S24–S25). The arsenic lone pair could be hybridized with the neighboring  $\pi$ -orbitals of the benzene rings that realized the global conjugation. Using these coplanar geometries, we also assessed the aromaticity in the  $S_0$  state with the NICS-scan plots (Figures S26–S27). The flattened arsepins **3-Me** and **3-Ph** showed distinct antiaromatic character (+7.6 and +11.7 ppm, respectively) at the global center of the arsepin rings, indicating the reversal of Hückel aromaticity.

**Table 2.** NICS(1) and HOMHED values of the arsepin cores of **3-Me** and **3-Ph** for the optimized structure in the  $S_0$  and  $S_1$  states.

	State	<b>3-Me</b>	<b>3-Ph</b>
NICS(1)/ ppm	$S_0$	–2.6	–1.2
	$S_1$	–6.7	–9.3
HOMHED	$S_0$	0.37	0.28
	$S_1$	0.89	0.90

In conclusion, novel dibenzo[*b,f*]arsepin derivatives, **3-Me** and **3-Ph**, were synthesized, and the photoexcited conformational changes between the boat-like structures and the coplanar geometries in the  $S_1$  state were investigated by experimental calculations. The emission profile for **3-Me** and **3-Ph** reflected the degree of planarization. According to the NICS scans, ACID maps,

and HOMHED values, **3-Me** and **3-Ph** have distinct aromaticity in the  $S_1$  states according to Baird's rule, in contrast to the nonaromatic nature in the  $S_0$  states. Moreover, the lone pairs of the arsenic atoms played a pivotal role in the construction of the  $8\pi$ -electron heteropin circuits. These novel class of arsepin molecules exhibiting drastic photodriven conformational change are not only promising candidates for stimuli-responsive materials but also allow for a deeper understanding of Baird aromaticity.

## Acknowledgments

The work in Tohoku was supported by the Research Program of "Dynamic Alliance for Open Innovation Bridging Human, Environment and Materials" in "Network Joint Research Center for Materials and Devices". The work in KIT was supported by JSPS KAKENHI, grant Number JP17H04577 (Coordination Asymmetry), to HI. The work in Kyushu was supported by JSPS KAKENHI, grant numbers JP19H04586 and JP19K05439, to MI.

**Keywords:** arsepin, lone pair, Baird's rule, excited-state aromaticity, aromatic indices.

- [1] a) F. A. L. Anet, *J. Am. Chem. Soc.* **1964**, *86*, 458–460; b) F. R. Jensen, L. A. Smith, *J. Am. Chem. Soc.* **1964**, *86*, 956–957; c) M. A. Battiste, M. W. Couch, R. Rehberg, *J. Phys. Chem.* **1977**, *81*, 64–67; d) Y. Nakadaira, R. Sato, H. Sakurai, *Organometallics* **1991**, *10*, 435–442; e) T. Nishinaga, Y. Izukawa, K. Komatsu, *J. Phys. Org. Chem.* **1998**, *11*, 475–477; f) K. Komatsu, *Eur. J. Org. Chem.* **1999**, 1999, 1495–1502; g) T. Nishinaga, Y. Izukawa, K. Komatsu, *Tetrahedron* **2001**, *57*, 3645–3656; h) L. G. Mercier, S. Furukawa, W. E. Piers, A. Wakamiya, S. Yamaguchi, M. Parvez, R. W. Harrington, W. Clegg, *Organometallics* **2011**, *30*, 1719–1729; i) K. Mouri, S. Saito, S. Yamaguchi, *Angew. Chem. Int. Ed.* **2012**, *51*, 5971–5975; *Angew. Chem.* **2012**, *124*, 6073–6077; j) Y. Tokoro, K. Tanaka, Y. Chujo, *Org. Lett.* **2013**, *15*, 2366–2369.
- [2] a) L. G. Mercier, W. E. Piers, M. Parvez, *Angew. Chem. Int. Ed.* **2009**, *48*, 6108–6111; *Angew. Chem.* **2009**, *121*, 6224–6227; b) A. Caruso, Jr., M. A. Siegler, J. D. Tovar, *Angew. Chem. Int. Ed.* **2010**, *49*, 4213–4217; *Angew. Chem.* **2010**, *122*, 4309–4313; c) R. E. Messersmith, M. A. Siegler, J. D. Tovar, *J. Org. Chem.* **2016**, *81*, 5595–5605; d) R. E. Messersmith, S. Yadav, M. A. Siegler, H. Ottosson, J. D. Tovar, *J. Org. Chem.* **2017**, *82*, 13440–13448; e) K. Schickedanz, J. Radtke, M. Bolte, H.-W. Lerner, M. Wagner, *J. Am. Chem. Soc.* **2017**, *139*, 2842–2851; f) Y. Adachi, J. Ohshita, *Organometallics* **2018**, *37*, 869–881.
- [3] K. Yoshida, T. Furuyama, C. Wang, A. Muranaka, D. Hashizume, S. Yasuie, M. Uchiyama, *J. Org. Chem.* **2012**, *77*, 729–732.
- [4] a) B. Quillian, Y. Wang, P. Wei, C. S. Wannere, P. R. Schleyer, G. H. Robinson, *J. Am. Chem. Soc.* **2007**, *129*, 13380–13381; b) T. Matsumoto, H. Takamine, K. Tanaka, Y. Chujo, *Org. Lett.* **2015**, *17*, 1593–1596.
- [5] D. Shukla, P. Wan, *J. Am. Chem. Soc.* **1993**, *115*, 2990–2991.
- [6] a) M. L. G. Borst, R. E. Bulo, C. W. Winkler, D. J. Gibney, A. W. Ehlers, M. Schakel, M. Lutz, A. L. Spek, K. Lammertsma, *J. Am. Chem. Soc.* **2005**, *127*, 5800–5801; b) V. Lyaskovskyy, R. J. A. van Dijk-Moes, S. Burck, W. I. Dzik, M. Lutz, A. W. Ehlers, J. C. Slootweg, B. de Bruin, K. Lammertsma, *Organometallics* **2013**, *32*, 363–373.
- [7] M. Rosenberg, C. Dahlstrand, K. Kilså, H. Ottosson, *Chem. Rev.* **2014**, *114*, 5379–5425.
- [8] N. C. Baird, *J. Am. Chem. Soc.* **1972**, *94*, 4941–4948.
- [9] a) D. H. Paik, D.-S. Yang, I.-R. Lee, A. H. Zewail, *Angew. Chem. Int. Ed.* **2004**, *43*, 2830–2834; *Angew. Chem.* **2004**, *116*, 2890–2894; b) T. L. Andrew, T. M. Swager, *Macromolecules* **2008**, *41*, 8306–8308; c) C.

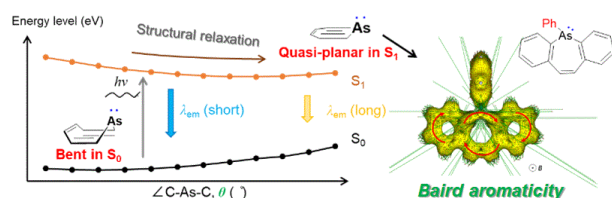
## COMMUNICATION

- Yuan, S. Saito, C. Camacho, S. Irle, I. Hisaki, S. Yamaguchi, *J. Am. Chem. Soc.* **2013**, *135*, 8842–8845; d) S. Saito, S. Nobusue, E. Tsuzaka, C. Yuan, C. Mori, M. Hara, T. Seki, C. Camacho, S. Irle, S. Yamaguchi, *Nat. Commun.* **2016**, *7*, 12094–12100; e) M. Ueda, K. Jorner, Y. Mo Sung, T. Mori, Q. Xiao, D. Kim, H. Ottosson, T. Aida, Y. Itoh, *Nat. Commun.* **2017**, *8*, 346–354; f) R. Kotani, H. Sotome, H. Okajima, S. Yokoyama, Y. Nakaike, A. Kashiwagi, C. Mori, Y. Nakada, S. Yamaguchi, A. Osuka, A. Sakamoto, H. Miyasaka, S. Saito, *J. Mater. Chem. C* **2017**, *5*, 5248–5256; g) M. Hada, S. Saito, S. Tanaka, R. Sato, M. Yoshimura, K. Mouri, K. Matsuo, S. Yamaguchi, M. Hara, Y. Hayashi, F. Röhrlich, R. Herges, Y. Shigeta, K. Onda, R. J. D. Miller, *J. Am. Chem. Soc.* **2017**, *139*, 15792–15800; h) T. Yamakado, S. Takahashi, K. Watanabe, Y. Matsumoto, A. Osuka, S. Saito, *Angew. Chem. Int. Ed.* **2018**, *57*, 5438–5443; *Angew. Chem.* **2018**, *130*, 5536–5541.
- [10] For reviews including structural transformation of heteroatom-containing compounds in the excited state, see: a) A. Wakamiya, S. Yamaguchi, *Bull. Chem. Soc. Jpn.* **2015**, *88*, 1357–1377; b) M. Gon, K. Tanaka, Y. Chujo, *Polym. J.* **2018**, *50*, 109–126; c) M. Gon, K. Tanaka, Y. Chujo, *Bull. Chem. Soc. Jpn.* **2019**, *92*, 7–18; d) M. Hirai, N. Tanaka, M. Sakai, S. Yamaguchi, *Chem. Rev.* in press (DOI: 10.1021/acs.chemrev.8b00637).
- [11] a) J. A. Kerr in *CRC Handbook of Chemistry and Physics*, 81st ed. (Ed.: D. R. Lide), Boca Raton, US, 2000; b) K. Naka, A. Nakahashi, M. Arita, Y. Chujo, *Organometallics* **2008**, *27*, 1034–1036; c) M. Ishidoshiro, Y. Matsumura, H. Imoto, Y. Irie, T. Kato, S. Watase, K. Matsukawa, S. Inagi, I. Tomita, K. Naka, *Org. Lett.* **2015**, *17*, 4854–4857; d) J. P. Green, S. J. Cryer, J. Marafie, A. J. P. White, M. Heeney, *Organometallics* **2017**, *36*, 2632–2636.
- [12] a) S. Yasuike, H. Ohta, S. Shiratori, J. Kurita, T. Tsuchiya, *J. Chem. Soc. Chem. Commun.* **1993**, *4*, 1817–1819; b) S. Shiratori, S. Yasuike, J. Kurita, T. Tsuchiya, *Chem. Pharm. Bull.* **1994**, *42*, 2441–2448.
- [13] a) E. Adams, D. Jeter, A. W. Cordes, J. W. Kolis, *Inorg. Chem.* **1990**, *29*, 1500–1503; b) B. Carison, G. D. Phelan, W. Kaminsky, L. Dalton, X. Jiang, S. Liu, A. K.-Y. Jen, *J. Am. Chem. Soc.* **2002**, *124*, 14162–14172.
- [14] a) J. W. B. Reesor, G. F. Wright, *J. Org. Chem.* **1957**, *22*, 382–385; b) P. S. Elmes, S. Middleton, B. O. West, *Aust. J. Chem.* **1970**, *23*, 1559–1570.
- [15] a) H. Imoto, K. Naka, *Main Group Strategies towards Functional Hybrid Materials*; T. Baumgartner, F. Jaekle, Eds.; John Wiley & Sons Ltd.: New York, US, 2018; Chapter 15, pp 383–403; b) H. Imoto, *Polym. J.* **2018**, *50*, 837–846; c) H. Imoto, K. Naka, *Chem. Eur. J.* **2019**, *25*, 1883–1894.
- [16] a) K. Naka, T. Umeyama, Y. Chujo, *J. Am. Chem. Soc.* **2002**, *124*, 6600–6603; b) T. Umeyama, K. Naka, A. Nakahashi, Y. Chujo, *Macromolecules* **2004**, *37*, 1271–1275; c) T. Kato, S. Tanaka, K. Naka, *Chem. Lett.* **2015**, *44*, 1476–1478; d) S. Tanaka, H. Imoto, T. Kato, K. Naka, *Dalton Trans.* **2016**, *45*, 7937–7940.
- [17] M. J. Mio, L. C. Kopel, J. B. Braun, T. L. Gadzikwa, K. L. Hull, R. G. Brisbois, C. J. Markworth, P. A. Grieco, *Org. Lett.* **2002**, *4*, 3199–3202.
- [18] CCDC 1905250 (**3-Me**), 1905252 (**3-Ph**), and 1905251 (**4**) contain the supplementary crystallographic data for this paper. These data are provided free of charge by The Cambridge Crystallographic Data Centre.
- [19] J. A. G. Drake, D. W. Jones, *Acta Cryst.* **1982**, *38*, 200–203.
- [20] This lower-energy photoluminescence was not detected in the solid state. See Figure S9 in SI.
- [21] a) B. Stevens, M. I. Ban, *Trans. Faraday Soc.* **1964**, *60*, 1515–1523; b) T. Matsumoto, H. Takamine, K. Tanaka, Y. Chujo, *Mater. Chem. Front.* **2017**, 2368–2375.
- [22] Emission lifetimes of **3-Me** were also measured (probed at 364 nm and 584 nm) as shown in Figure S8. However, the intensity of the longer-wavelength emission was insufficient to analyze the dynamics of **3-Me** in the S<sub>1</sub> state.
- [23] The lack of discernable phosphorescence might be considered by less substantial orbital participation from the heavier arsine atom in LUMO of **3-Ph**.
- [24] The calculations were conducted under vacuum condition. We also carried out the calculation for **3-Ph** under hexane and DMSO conditions (Figure S23) to confirm that the solvent effects can be ignored in the present case.
- [25] C. P. Frizzo, M. A. P. Martins, *Struct. Chem.* **2012**, *23*, 375–380.
- [26] The semiempirical parameters for C–As bond were used according to the literature. See reference 11d.
- [27] To verify the substitution effect of the heteroatom on the aromaticity of the 8π heteropin cores, the same calculations were conducted for the dibenzo[*b,f*]azepin and phosphepin derivatives. For details, see SI (Figures S28–S29).

## COMMUNICATION

## Entry for the Table of Contents

## COMMUNICATION



Dibenzosepins possessing formally  $8\pi$ -electron systems showed highly bent structures in the ground states, while quasi-planar structures were favored in the singlet excited states. The drastic conformational change upon photo-excitation was studied based on Baird's rule.

I. Kawashima, H. Imoto, M. Ishida, H. Furuta, S. Yamamoto, M. Mitsuishi, S. Tanaka, T. Fujii, K. Naka\*

Page No. – Page No.

**Dibenzosepins: Planarization of  $8\pi$  system in the Lowest Singlet Excited State**